Simulation of Self-Assembled Monolayers under Normal Stress

Redhouane Henda
Chemical Engineering Dept., King Saud University, Riyadh 11421, Saudi Arabia

Self-assembled monolayers (SAMs) are dense molecular assemblies with a two-dimensional order, which are formed by spontaneous chemisorption of functional long-chain hydrocarbon molecules, essentially alkane chains, on a solid surface (Ulman, 1991). At one end of the molecules composing a SAM is a head group with a strong preferential adsorption to the surface used, and at the other end a variety of tail groups can be affixed, thus altering dramatically the properties of the resulting surface. As an example, the wettability of a surface can be controlled with good precision by adsorbing, onto the surface, a SAM to which either a hydrophobic or a hydrophilic tail group has been affixed. The same strategy, by attaching different terminal groups to a SAM, can be used to control other properties of the surface, such as adhesion, lubrication, friction, and corrosion. Moreover, the understanding of the structure–property relationships in these systems (SAMs) is crucial for any progress in the development of new materials and engineering of their properties through the molecular-design approach. This importance has triggered much interest in the mainstream of chemistry, chemical engineering, and material science throughout the past few years (Ulman, 1991, 1995; Whitesides et al., 1993; Delamarche et al., 1994; Poirier and Tarlov, 1994; Liu and Salmeron, 1994; Grunze and Pertsin, 1997). Aside from experimental work, a number of simulations elucidating the structure and phase behavior of SAMs on the molecular level have been reported (Ulman et al., 1989; Sellers et al., 1993; Hautman and Klein, 1989, 1990; Hautman et al., 1991; Siepmann and McDonald, 1993a; Mar and Klein, 1994; Pertsin and Grunze, 1996). A few simulations have also been undertaken to probe their response to compressive loads (Siepmann and McDonald, 1993b; Tupper et al., 1994; Siepmann, 1995). The mechanical properties of substrate-supported organic monolayers such as SAMS are strongly related to the tribological properties of these systems. Also, the study of the response of SAMs to external loads can provide valuable hints as to their performance in service.

In both Monte Carlo (MC) (Siepmann and McDonald, 1993b; Siepmann, 1995) and molecular dynamics (MD) (Tupper et al., 1994) simulations of the mechanical relaxation of SAMs, the interaction model used to describe the monolayer was based on the united-atom approximation. That is, the alkanethiol chains were modeled using pseudoatoms representing the CH_2 and CH_3 groups. In the MC calculations, the interaction potential between the pseudoatoms and substrate was solely dependent on the pseudoatom–substrate separation, that is, the gold surface was assumed to be absolutely smooth. In contrast, surface corrugation was emphasized and accomplished by including explicit gold atoms in the MD simulations. The results obtained by MC and MD simulations provided valuable information as to the response of a SAM to compression, but many important relevant questions remained unanswered. Of primary importance is the question relative to the sensitivity of the calculated properties to variations in the force field. This interest is driven by the fact that the force fields used to simulate SAMs are very approximate and simplified. Another problem, which is closely related to the choice of force field, is the issue of the equilibrium monolayer configuration. The available force fields (at least the ones used in the cited simulation work) fail to correctly predict the equilibrium configuration of the alkanethiol/Au (111) SAMs. The most favorable calculated structure proves to be a herringbone structure with two symmetrically distinct chains in the unit cell, whereas diffraction (Camilone et al., 1993; Fenter et al., 1993) and STM (Anselmetti et al., 1994; Delamarche et al., 1996) experiments reveal a unit cell containing four independent cells. The existence of nonequivalent adsorption sites was also revealed in SFG and grazing incidence X-ray measurements (Yeganeh et al., 1995; Fenter et al., 1994). The question is then to what extent can the equilibrium structure affect the response of a SAM to compression?

In this work, we report on the response of SAMs to compression, calculated with different force fields and monolayer configurations in the unit cell. Since the MD and MC techniques are computationally too expensive to perform such calculations, we resort to the static-energy minimization technique (Pertsin and Kitaigorodsky, 1987). The use of this technique, which provides quantities related to zero temperature, is justified for two reasons. First, we are mainly interested in *changes* in the properties of SAMs due to variations in the force field used to calculate the stable structures, and so on,

and not in the absolute values of these properties. Second, since we are also interested in the mechanical properties of SAMs, by analogy with organic crystals (Kitaigorodsky, 1973), it can be expected that the static terms give a dominant contribution to the elastic properties of SAMs. The comparative calculations are performed with a $CH_3(CH_2)_{17}SH/Au(111)$ SAM. In addition, for one selected force field and monolayer configuration we probe the effect of the chain length (or thickness) of SAM films, formed by C_n ($n = 5, 8, 10, 28$) homologues, on the response of a SAM to compression.

Model

The force fields tried are two all-atom force fields, which correspond to force fields I and IV used by Pertsin and Grunze (1994), and also a united-atom force field (hereafter, force field U). In all three force fields, the conformational energy of the alkanethiol chain is evaluated as the sum of bond-angle bending, torsional, and nonbonded contributions using the same potentials as employed in computer simulations of SAMs (Hautman and Klein, 1989, 1990; Hautman et al., 1991; Siepmann and McDonald, 1993a). The bonds of the alkanethiol chain are treated as rigid. The bond-length constraints are incorporated via a rotational displacement algorithm described elsewhere (Pertsin and Grunze, 1994). In all force fields, the interaction of the CH_2 and CH_3 groups with the gold substrate is modeled with the 3-12 potential suggested by Hautman and Klein (1989, 1990), Hautman et al. (1991), and Siepmann and McDonald (1993a). The all-atom force fields I and IV treat the interchain interactions using Buckingham 6-exp potentials, with available parametrizations for sulfur, carbon, and hydrogen (Pertsin and Grunze, 1994). In the united-atom force field U, use is made of the same potential functions as employed in the simulations of the mechanical relaxation (Siepmann and McDonald, 1993b; Tupper et al., 1994; Siepmann, 1995).

In general, the interaction of the sulfur head group with the gold surface involves three contributions. The first is responsible for the distance dependence and is described with a 3-12 potential. The second contribution represents an Au–S–C angle bending term. The third contribution is a surface corrugation potential, which describes the energy changes associated with lateral displacement of the head group. The analytical forms and parameters of these contributions are listed in Table 1. The 3-12 potential is common to all the tried force fields. In force fields I and U, the Au–S–C angle is not subject to any bending potential, and the surface corrugation is described by a truncated expansion of the sulfur–substrate interaction energy in the reciprocal lattice vectors. The extent of surface corrugation is specified by the peak-to-valley roughness parameter b. Force field IV is based on *ab initio* quantum chemical data reported by Sellers et al. (1993) for the interaction of a methylthiol molecule with a gold cluster. This force field includes a nonzero Au–S–C bending term and a harmonic corrugation potential, for the interaction of the head group with the substrate, whose parameters are fitted to the *ab initio* data. Depending on the value of the Au–S–C angle, the force constant and equilibrium angle of the bending potential are switched between the respective values found for *sp*3 and *sp* hybridized states of the sulfur atom.

Table 1. Parameters of the Surface Corrugation and Au–S–C Angle-Bending Potentials for Force Fields I and IV*

Potentials, Parameters	I	IV
Au–S–C angle bending	—	$1/2\,k_b(\alpha - \alpha_0)^2$
Surface corrugation	$b\left[3 - \sum_{i=1}^{3} \cos(s \cdot k_i)\right]/4.5$	$1/2\,k_c(d - d_0)^2$
b(kcal·mol^{-1})	2	—
k_b(kcal·mol^{-1}·rad^{-2})	—	11.6/0.72
α_0(deg)	—	99.5/180
k_c (kcal·mol^{-1}·Å^{12})	—	10.5
d_0 (Å)	—	0.27
k_i (Å^{-1}): reciprocal Lattice vectors	$k_0(\sqrt{3}/2, -1/2)$, $k_0(-\sqrt{3}/2, -1/2), (0, 1)$	—

*The same Lennard-Jones 3-12 potential was used for the distance-dependent sulfur–gold interaction. The parameter k_0 is equal to 1.448.

In the present simulation of the dependence of SAM properties on the monolayer configuration, the ten lowest-energy configurations, corresponding to ten local energy minima found on the energy hypersurface of the $CH_3(CH_2)_{17}SH/Au(111)$ SAM (Pertsin and Grunze, 1994), are considered. These are two configurations whose unit cell contains one symmetrically independent chain ($N = 1$, models 1-1 and 1-2), four lowest-energy configurations with $N = 2$ (models 2-1 to 2-4), and four lowest-energy configurations with $N = 4$ (models 4-1 to 4-4). Each configuration is specified by tilt and precession angles, θ and ψ, which describe the orientation of the chain axes; N twist angles, φ, which specify rotation of the chains around their axes; and $3N$ Cartesian coordinates, x, y, and z, which show the positions of the chains in the unit cell. The chain conformation is initially assumed to be planar *all-trans* zigzag.

The compression of a SAM film is accomplished in the following way. A low-energy configuration is taken as the starting point and its energy is minimized in two steps. At the first step, the alkanethiol chains are treated as rigid and the potential energy of the monolayer is minimized with respect to all of the aforementioned configurational parameters except for θ. At the second step, the rigid-body approximation is removed and the configuration is allowed to relax with respect to both the rigid-body and intramolecular degrees of freedom. The only constraint incorporated at this step is that the z-coordinate of the carbon atom in the terminal CH_3 group is kept fixed at the value found in the rigid-body search. It is this fixed value of z that is taken as the definition of the current monolayer thickness h. Then the tilt angle θ is incremented (or decremented, in the case of decompression) by some $\Delta\theta$, and the two-step minimization procedure is again accomplished starting with the lowest-energy configuration found before. As a result, we obtain the lowest-energy monolayer configuration and the respective potential energy as a function of θ (and also of h). The compressive load corresponding to a particular h is easily calculated as the derivative of the potential energy with respect to h. The normal stress is calculated by relating the load per chain to the relevant surface area (21.7 Å^2), while the strain is determined as $(h - h_0)/h_0$, where h_0 is the thickness at zero stress. The uniaxial Young modulus, E, is then found as the slope of the stress–strain curve at zero strain.

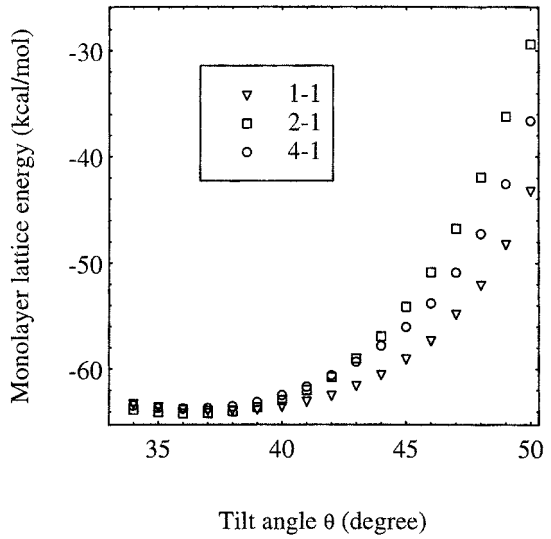

Figure 1. Simulated potential energy of the lowest energy $N = 1, 2, 4$ monolayer models as a function of the tilt angle.

Results and Discussion

A typical curve showing the dependence of the monolayer energy on the tilt angle is depicted in Figure 1. The data reported in this figure and in the following figures, unless other stated, refer to octadecanethiol and were obtained using force field I. The energy minimum on each curve in Figure 1 corresponds to the calculated equilibrium tilt angle at zero load. The tilt angles to the right of the minimum refer to compressed monolayers, while the angles to the left are formally related to negative loads, that is, to a situation where the monolayer is stretched along the normal to the surface. Two points are worth noting in Figure 1. That is, the two-chain unit cell structure has the lowest lattice energy, compared to one- and four-chain unit cells, and is therefore the most stable monolayer model when no load is applied. And as the monolayer is subjected to loads, less energy is needed to compress the structure with one chain per unit cell, in comparison with the other two structures. This lower resistance to compressive loads exhibited by the monolayer model with $N = 1$ can be expected, since all the chains in the unit cell have the same orientation and are rotated about the same value around their axes. In the case of the monolayer models with $N = 2$ and $N = 4$, the chains in the unit cell present different rotation angles around their respective axes, and they therefore develop an additional resistance to the applied loads in order to accommodate their rotation mismatch. It is also striking to notice that the monolayer model with $N = 4$ was not the less compressive structure as might be expected. This is due to the fact that in the lowest-energy configurations the four symmetrically independent chains in model 4-1 degenerated into two distinct pairs of identical chains to give a two-chain unit-cell structure. Moreover, the response of model 4-1 to compression shows a special feature for loads corresponding to tilt angles higher than 43° and will be explained later.

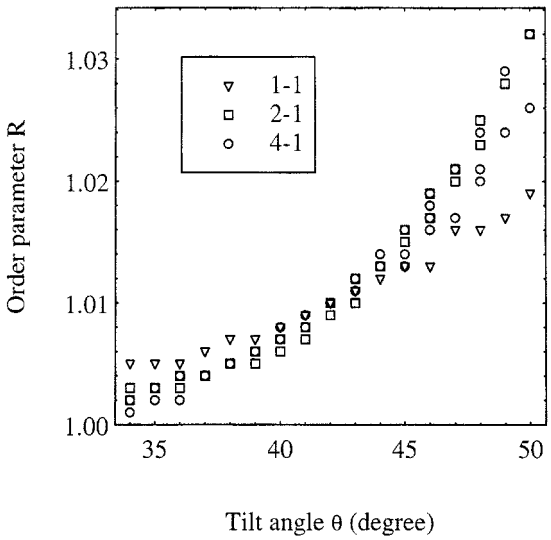

Figure 2. Order parameter of the molecular chains in the lowest energy $N = 1, 2, 4$ monolayer models as a function of molecular tile.

All molecules are represented.

In general, the compressive load did not produce significant structural changes, so that the monolayer configuration retained its characteristic features. First, compression led to negligible deviations from the conformational parameters of the uncompressed monolayer. The largest change in bond angles along the chain was about 3° and noticed for the S−C−C angle. The torsion angles along the chain were also almost unchanged. A convenient way to capture the changes in torsion angles along the chain backbone, but excluding the terminal group angles, during compression can be obtained through the determination of the order parameter R defined by Hautman and Klein (1989, 1990). For an all-trans molecule, that is, for a planar molecule, R is equal to unity. The order parameter is other than unity if the molecule plane is not well defined, because of some deviation from the all-trans conformation. From Figure 2, which is typical to all monolayer models investigated, it is clear that the chains retained their planarity during compression. A maximum shift of 8° from the all-trans value was noticed for the torsion angles of the terminal groups. The only exception was structure 4-1, where the torsion angle of the head group changed by 23° from the all-trans value. This can be seen in Figure 3, which presents the dependence of the head group torsion angle $S-C_1-C_2-C_3$ on the tilt angle. In Figure 3, the head-group torsion angles of two out of the four molecules exhibit a dramatic change around, viz., an inflexion point at, a tilt angle value of 45°. This inflexion corresponds to about the same tilt angle from which the energy-tilt angle curve of model 4-1 presents a special feature referred to earlier in Figure 1. And it appears that this conformational change in the vicinity of the molecular heads has a damping effect on the applied load (Figure 1). The Au−S−C angle could not of course remain unaffected by compression because it was closely related to the tilt angle by the computation algorithm. As a result, the changes in the Au−S−C angle were about 10° at the end of compression ($\theta = 50°$). Second, the configurational parameter, viz., precession ψ and twist φ angles, of the monolayers with $N = 2$ and $N = 4$ were not substantially affected by

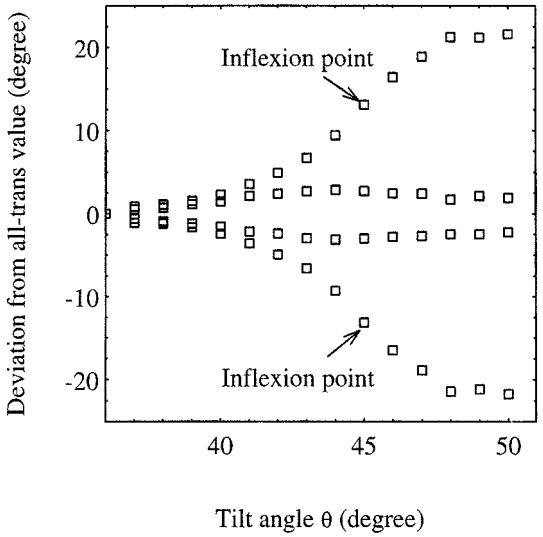

Figure 3. Dependence of the deviation from all-trans value of the equilibrium torsion angle $S-C_1-C_2-C_3$ on molecular tilt for model 4-1.

The four molecules are represented.

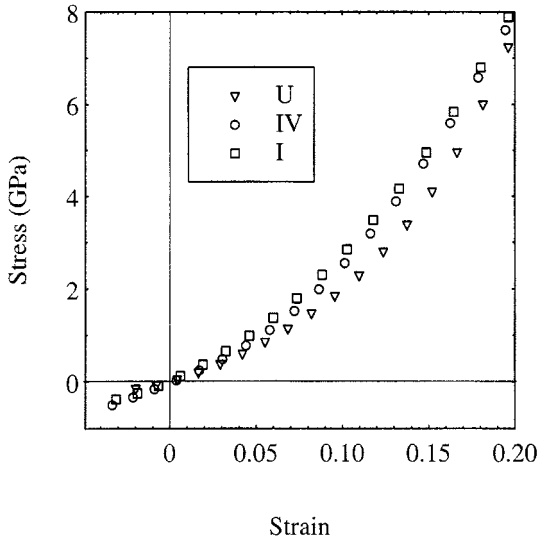

Figure 4. Stress–strain curves for model 2-1 calculated using different force fields.

The solid lines are given as guides.

compression (change by max. 5°). More appreciable changes were observed in the simplest $N = 1$ systems. Thus, in model 1-1 the change in the twist angle φ reached 15° at the end of compression.

The effect of the monolayer configuration on its mechanical properties can be appreciated through examination of the Young's modulus of the different monolayer models. For force field I, for example, the Young's modulus is 12.0 GPa for model 1-1, 16.0 GPa for model 2-1, and 18.3 GPa for model 4-1. This variation provides an idea of the error that can be involved in the calculated mechanical constants of the monolayer because of the lack of exact knowledge of its equilibrium structure. The calculated Young's modulus for the different monolayer models using force fields I and IV did not differ significantly, the largest deviation being 12% for model 2-4. This means that the explicit Au–S–C bending term, although it offers additional resistance to compression, does not play a significant role in the mechanical properties. A much more pronounced effect is observed on going from the all-atom force fields I and IV to the united-atom force field U, as shown in Figure 4. Thus, the Young's modulus of model 2-1 corresponding to the global energy minimum falls from 16.0–15.0 to 9.9 GPa when the all-atom force fields are replaced by the united-atom one. The observed changes in the values of the Young's modulus are associated, at least in part, with differences in the equilibrium monolayer structures resulting from the all-atom and united-atom force fields. For example, at low strains, which are important for calculation of the Young's modulus, model 1-1 has the equilibrium precession angle ψ around 20° and the equilibrium twist angle φ around $-130°$, when treated using force fields I and IV. With force field U, the energy minimum corresponds to $\psi \approx 4°$ and $\varphi \approx -95°$; that is, the calculated Young's modulus of model 1-1 refers to a substantially different monolayer structure.

An estimate of the Young's modulus from the interfacial-force microscopic data (Joyce et al., 1992), related to the mechanical relaxation of hexadecathiol/Au(111) SAM, gives a value of about 5 GPa. This is, of course, a gross value, because in the cited work the contact area produced by the tungsten tip was approximately estimated by simple Hertzian elastic analysis. Also, when a SAM is relaxed at the end of the compression half-cycle, it recovers from the deformation, and no mechanical hysteresis has been reported within the conditions of the present work.

The stress–strain curve calculated for a particular monolayer configuration proved to be practically independent of the length of the alkanethiol chain for a number of carbon monomer units along a chain backbone larger than 7 (Figure 5). This is supported by the Young's modulus data of C_8, C_{10},

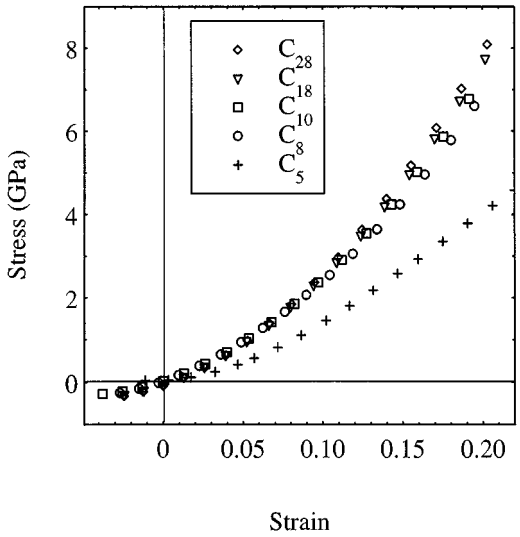

Figure 5. Dependence of the stress strain curves of model 2-1 on the number of monomer units (C_n) along a molecular-chain backbone.

The solid lines are given as guides.

C_{18}, and C_{28} SAM films calculated for model 2-1 using force field IV (13.2, 14.7, 15.0, and 15.5 GPa, respectively), and from their stress–strain curves. This result is explained by the fact that no structural changes were noticed as more alkyl backbone units were subtracted from C_{28}. From Figure 5, the C_5 SAM film appears to be much softer ($E = 2.0$ GPa) than the longer C_n homologues. A similar trend has been noticed in the other structures. The precise cause of the mechanical behavior of C_5 SAM film is not clear, but the value of the torsion angle of the tail group of this monolayer was found to differ by 12° from the values of the torsion angles of the tail groups of the longer homologues during compression (although the difference is quite small).

Conclusions

In this study, we probed the response of alkanethiol/Au(111) SAMs to compression in terms of load-induced structural changes and film Young's modulus, using the static-energy minimization technique. The monolayer response was found to depend on the assumed monolayer configuration in the unit cell, the force field used, and the chain length of C_n homologues for $n < 8$. Our findings show that the calculated Young's modulus may be at least a factor of 2 in error, due to uncertainties in the available force fields and the lack of exact knowledge of the equilibrium monolayer.

Acknowledgments

This work was supported by the Deutsche Forschungsgemeinschaft (Germany) through SFB 359, the U.S. Office of Naval Research under Grant 00014-94-1-0492, and the Alexander von Humboldt-Stiftung (Germany). M. Grunze and A. Pertsin are gratefully acknowledged for stimulating discussions.

Literature Cited

Anselmetti, D., A. Baratoff, H.-J. Guntherodt, E. Delamarche, B. Michel, H. Gerber, H. Wolf, and H. Ringsdorf, "Domain and Molecular Superlattice Structure of Dodecanethiol Self-Assembled on Au(111)," *Europhys. Lett.*, **27**, 365 (1994).

Camilone, N., C. E. D. Chisdey, G.-Y. Liu, and G. J. Scoles, "Superlattice Structure at the Surface of a Monolayer of Octadecanethiol Self-Assembled on Au(111)," *J. Chem. Phys.*, **98**, 3503 (1993).

Delamarche, E., B. Michel, Ch. Gerber, D. Anselmetti, H.-J. Guentherodt, H. Wolf, and H. Ringsdorf, "Real-Space Observation of Nanoscale Molecular Domains in Self-Assembled Monolayers," *Langmuir*, **10**, 2869 (1994).

Delamarche, E., B. Michel, H. A. Biebuyck, and C. Gerber, "Golden Interfaces: The Surface of Self-Assembled Monolayers," *Adv. Mater.*, **8**, 719 (1996).

Fenter, P., A. Eberhardt, and P. Eisenberger, "Self Assembly of n-Alkyl Thiols as Disulfides," *Science*, **266**, 1216 (1994).

Fenter, P., P. Eisenberger, and K. S. Liang, "Chain-Length Dependence of the Structures and Phases of $CH_3(CH_2)_{n-1}SH$ Self-Assembled on Au(111)," *Phys. Rev. Lett.*, **70**, 2447 (1993).

Grunze, M., and A. Pertsin, "Two Simple Models for Computer Simulation of Self-Assembled Monolayers," *J. Mol. Catal. A*, **119**, 113 (1997).

Hautman, J., and M. L. Klein, "Simulation of a Monolayer of Alkyl Thiol Chains," *J. Chem. Phys.*, **91**, 4994 (1989).

Hautman, J., and M. L. Klein, "Molecular Dynamics Simulation of the Effects of Temperature on a Dense Monolayer of Long-Chain Molecules," *J. Chem. Phys.*, **93**, 7483 (1990).

Hautman, J., J. P. Bareman, W. Mar, and M. L. Klein, "Molecular Dynamics Investigations of Self-Assembled Monolayers," *J. Chem. Soc. Faraday Trans.*, **87**, 2031 (1991).

Joyce, A., R. C. Thomas, J. E. Houston, T. A. Michalske, and R. M. Crooks, "Mechanical Relaxation of Organic Monolayer Films Measured by Force Microscopy," *Phys. Rev. Lett.*, **68**, 2790 (1992).

Kitaigorodsky, A. I., *Molecular Crystals and Molecules*, Academic Press, New York (1973).

Liu, G.-Y., and M. B. Salmeron, "Reversible Displacement of Chemisorbed n-Alkane Thiol Molecules on Au(111) Surface: An Atomic Force Microscopy Study," *Langmuir*, **10**, 367 (1994).

Mar, W., and M. L. Klein, "Molecular-Dynamics Study of the Self-Assembled Monolayer Composed of $S(CH_2)_{14}CH_3$ Molecules Using an All-Atoms Model," *Langmuir*, **10**, 188 (1994).

Pertsin, A. J., and A. I. Kitaigorodsky, *The Atom-Atom Potential Method*, Springer-Verlag, Berlin (1987).

Pertsin, A. J., and M. Grunze, "Low Energy Structures of a Monolayer of Octadecanethiol Self-Assembled on Au(111)," *Langmuir*, **10**, 3668 (1994).

Poirier, G. E., and M. J. Tarlov, "The C(4×2) Superlattice of *n*-Alkanethiol Monolayers Self-Assembled on Au(111)," *Langmuir*, **10**, 2853 (1994).

Sellers, H., A. Ulman, Y. Shnidman, and J. E. Eilers, "Structure and Binding of Alkyl Thiolates on Gold and Silver Surfaces: Implications for Self-Assembly," *J. Amer. Chem. Soc.*, **115**, 9389 (1993).

Siepmann, J. I., "Monte Carlo Calculations for the Mechanical Relaxation of a Self-Assembled Monolayer and for the Structures of Alkane/Metal Interfaces," *Tribology Lett.*, **1**, 191 (1995).

Siepmann, J. I., and I. R. McDonald, "Domain Formation and System-Size Dependence in Simulations of Self-Assembled Monolayers," *Langmuir*, **9**, 2351 (1993a).

Siepmann, J. I., and I. R. McDonald, "Monte Carlo Simulation of the Mechanical Relaxation of a Self-Assembled Monolayer," *Phys. Rev. Lett.*, **70**, 453 (1993b).

Tupper, K. J., R. J. Colton, and D. W. Brenner, "Simulations of Self-Assembled Monolayers Under Compression: Effect of Surface Asperities," *Langmuir*, **10**, 2041 (1994).

Ulman, A., *An Introduction to Ultrathin Organic Films: From Langmuir-Blodgett to Self-Assembly*, Academic Press, Boston (1991).

Ulman, A., "Surface Absorption of Monolayers," *MRS Bull.*, **20**, 46 (1995).

Ulman, A., E. J. Eilers, and N. Tilman, "Packing and Molecular Orientation of Alkanethiol Monolayers on Gold Surfaces," *Langmuir*, **5**, 1147 (1989).

Whitesides, G. M., G. S. Ferguson, D. Allara, D. Scherson, L. Speaker, and A. Ulman, "Organized Molecular Assemblies," *Crit. Rev. Surf. Chem.*, **3**, 49 (1993).

Yeganeh, M. S., S. M. Douglas, R. S. Polizzotti, and P. Rabinowitz, "Interfacial Atomic Structure of a Self-Assembled Alkyl Thiol Monolayer/Au(111): A Sum-Frequency Generation Study," *Phys. Rev. Lett.*, **74**, 1811 (1995).

Manuscript received Apr. 16, 1999, and revision received Nov. 1, 1999.